



STRUCTURAL AND ELECTRICAL PROPERTIES OF M-TYPE SUBSTITUTED CALCIUM HEXAFERRITES

S. R. Gawali¹, P. R. Moharkar², R. R. Kherani³ and K. G. Rewatkar⁴

¹Dr. Ambedkar College, Chandrapur, (M.S.), India (442401)

²A. C. S. College, Chandrapur, (M.S.), India (442401)

³Shree Shivaji College, Rajura, (M.S.), India (442905)

⁴Dr. Ambedkar College, Nagpur, (M.S.), India (440010)

sanjaygawali500@gmail.com

Abstract:

The series of samples of aluminium substituted calcium hexaferrite with composition $\text{CaAl}_x\text{Fe}_{12-x}\text{O}_{19}$ ($x=1$ and 3) were synthesized by microwave induced sol-gel combustion method. X-ray powder diffraction (XRD) patterns of all prepared samples indicated the formation a single M-type phase hexagonal ferrite. The lattice constants, cell volume, X-ray density, bulk density and porosity of samples were measured from XRD data. TEM analysis revealed that the average particle size of the samples are in nano-range. The dc electrical resistivity, activation energy and drift mobility of substituted calcium ferrites were investigated as a function of temperature and Al^{3+} ion concentration. The enhanced resistivity of the aluminium substituted calcium hexaferrite has a potential application in microwave devices. The drift mobility of samples was calculated from the electrical resistivity data. The effect of aluminium ion substitution on electric properties of nano-ferrites was explained on the basis of cation distribution in the crystal structure.

Keywords: M-type hexagonal ferrite, structural property, electrical property, drift mobility, Sol-gel combustion method etc.

Introduction:

The materials that have dimensions in the nanometer regime may possess surprising properties that might be very different from those of their bulk counterparts. The nano-materials bridge the gap between bulk material and an isolated atom in its physical and chemical properties [1]. The researchers always attempt to invent new nano materials which could directly or indirectly be used with a little improvisation into the makings of advanced electronics nano gadgets [2]. The gadgets include nanomemory in nanobots, magnetic storage in set top box in satellite communication, HDTV, high-density magnetic tapes, floppy disks, high-coercivity magnetic media, analog and digital recorders, data retrievers, etc. For such electronics gadgets, magnetic material with nanoscaled particles with very special magnetic traits is the foremost requirement. M-type calcium hexaferrite $\text{CaFe}_{12}\text{O}_{19}$ has been intensively studied as a material for permanent magnets, high-density magnetic recording media and microwave devices [3–4].

In current research, the samples of M-type aluminium substituted calcium hexaferrite have been synthesized by sol-gel combustion method. The effect of Al^{3+} ion for Fe^{3+} ion on structural and electrical properties of doped calcium hexaferrite have been investigated.

Experimental

Sample preparations

The aluminium substituted calcium hexaferrite powders with composition $\text{CaAl}_x\text{Fe}_{12-x}$

O_{19} ($x=1$ and 3) have been synthesized by microwave induced sol-gel combustion method. The synthesis method involved the combustion of redox mixtures, in which metal nitrates acted as an oxidizing reactant and urea as a reducing reactant. The initial composition of solution containing metal nitrates and urea was based on the total oxidizing and reducing valences of the oxidizer and the fuel using the concept of propellant chemistry [5].

The stoichiometric amounts of AR grade $\text{Ca}(\text{NO}_3)_2 \cdot 4\text{H}_2\text{O}$, $\text{Fe}(\text{NO}_3)_3 \cdot 9\text{H}_2\text{O}$ and $\text{Al}(\text{NO}_3)_3 \cdot 9\text{H}_2\text{O}$ and urea $\text{CO}(\text{NH}_2)_2$, dissolved in a minimum quantity of water, were placed in a beaker. The solutions as prepared in beaker were mixed together to form a homogeneous transparent aqueous solution. The aqueous solution was then heated into the micro-wave oven. After few minutes aqueous solution get converted into wet gel by evaporating the water. After the wet gel reaches the point of spontaneous combustion, it begins burning and becomes a solid which burns at a temperature above 1000°C . The combustion is not completed until all the flammable substances are consumed and the resulting material is a loose, highly friable substance exhibiting voids and pores formed by escaping gases during combustion reaction. The ash of aluminium substituted calcium ferrite was obtained after complete combustion. This ash was then ground in agate mortar and then pressed into pellets using PVA as binder. These pellets were finally annealed at 950°C for 2 hour at a heating rate of $5^\circ\text{C}/\text{min}$.

Characterization

The phase identification of samples were carried out by using a Philips X-ray diffractometer (PW-1710) and Cu-K α radiation with the wavelength $\lambda = 1.54056 \text{ \AA}$. The X-ray pattern showed the formation of a single phase of M-type hexagonal ferrite without any impurity. The values of lattice constant 'a' and 'c', the unit cell volume (V), X-ray density ($\rho_{x\text{-ray}}$), bulk density (ρ_m) and porosity (P) were calculated by using following equations.

$$\frac{1}{d^2} = \frac{4(h^2+hk+k^2)}{3a^2} + \frac{l^2}{c^2} \quad (1)$$

$$V = 0.8666a^2c \quad (2)$$

$$\rho_{x\text{-ray}} = \frac{ZM}{N_A V} \quad (3)$$

$$\rho_m = \frac{m}{(\pi r^2)h} \quad (4)$$

$$P = 1 - \frac{\rho_m}{\rho_{x\text{-ray}}} \quad (5)$$

where, 'a' and 'c' are lattice constants, 'M' is the molar mass, 'm' is the mass of pellet, 'r' is radius of the pellet, 'N_A' is Avogadro's number and 'V' is the unit cell volume.

The average particle size of synthesized samples were determined by a Transmission Electron Microscope (TEM).

As these ferrites have very high resistivity, so the four probe method was employed to study DC electrical resistivity of the said ferrites system in the temperature range 300K to 873 K. The DC electrical resistivity of all the samples decreases with increasing temperature in accordance with Arrhenius equation[6]

$$\rho = \rho_0 \exp\left(\frac{\Delta E}{k_B T}\right) \quad (6)$$

where, 'k_B' is the Boltzmann constant, 'T' is temperature and 'ΔE' is the activation energy, which is the energy needed to release an electron from the ion for a jump to neighbouring ion, giving rise to the electrical conductivity.

The activation energy of the aluminium substituted calcium hexaferrites have been determined from the slope of plots of ln(σ) versus temperature (1000/T) above and below the transition temperature (T_v).

The drift mobility (μ_d) of all synthesized hexaferrite samples were calculated using the relation[6]

$$\mu_d = \frac{1}{ne\rho} \quad (7)$$

where, 'e' is the charge on the electron, 'ρ' is the D.C. electrical resistivity at a given

temperature and 'n' is the concentration of charge carriers and can be calculated from the relation[6]

$$n = \frac{N_A \rho_m P_{Fe}}{M} \quad (8)$$

where 'N_A' is the Avogadro's number, 'ρ_m' is the bulk density, 'M' is the molecular weight of the sample, 'P_{Fe}' is the number of iron atoms in the chemical formula.

Results and Discussion:

XRD analysis

The XRD patterns of the samples are shown in Fig 1. The crystallographic data are tabulated in Table 1. The XRD data are analyzed by using computer software PCPDF Win, PowderX and FullProf Suite. By comparing the patterns with JCPDS, the phases in the different samples are determined. It was observed that all peaks were perfectly matched with standard pattern, confirming the single magnetoplumbite phase in the reported samples. The space group for the samples is observed to be SG: P6₃/mmc (No. 194). XRD pattern also show few noisy peaks which may be due to two reasons, firstly, the crystallite size are very small, secondly, it may be due to instrumental error.

The lattice constants (a) and (c) and (V) slightly changes with substitution of Al³⁺ ion in calcium hexaferrite sample. The decrease in cell volume is due to relatively large ionic radius of Al³⁺ ion (0.53 Å) comparing to that of Fe³⁺ ion (0.64 Å) for six fold coordination. These results agree well to that reported by Ounnunkad and Winotai [7] and Haneda and Kojima [8] for Cr substituted barium ferrite. The similar trend of lattice parameter and cell volume was also reported by Sang Won Lee [9] for La-Zn substituted Strontium ferrite. Rewatkar et al.[10] reported the similar values of lattice constants a and c.

TEM analysis

Fig. 2 shows TEM micrographs of aluminium substituted calcium hexaferrite. The average particle size of the samples is in nanorange with an average diameter of 94 nm. The TEM analysis shows remarkable changes in the microstructure, grain size and homogeneous particle size distribution. Therefore it could be attributed that these remarkable changes are observed as a perturbation of many dependant parameters like time of synthesis, temperature, process of annealing, intermittent quenching and grinding etc [11-12].

It showed that the resistivity of the prepared aluminium substituted calcium hexaferrites decreased with increasing temperature for each sample. This proved the

semiconductor nature of synthesized samples. Verwey's hopping mechanism helps to clarify that the change in mobility of charge concentration with increasing temperature was because of jumping or hopping from one Fe^{3+} ion to the next. The hopping probability increased with an increase in temperature, which resulted in the conductivity of the prepared materials [13]. In the crystal structure of hexaferrites, oxygen anions surrounded the cations on either octahedral sites or tetrahedral sites. Hexaferrites contain 64 ions per unit cell on 11 different symmetrical sites. The 24 iron ions are distributed over five distinct sites: three octahedral (B-sites), one tetrahedral (A-site) and one bipyramidal (C-site) [14–16]. The distance between two metal ions at the B-site is smaller than the distance between metal ions at the B-site and another metal ion at the A-site. Thus the electron hopping between A and B sites

under normal conditions has a small probability compared to B–B site hopping. Hopping between A–A sites is negligible for the simple reason that there are only Fe^{3+} ions at the A-site and any Fe^{2+} ions formed during processing preferentially occupy B-sites only [17].

Table 2 shows that dc electrical resistivity as well as activation energy (E) increased, while the drift mobility decreased with increasing concentration of Al^{3+} ions. The greater ionic radii and high resistive behaviour of aluminium ions act as an energy barrier for the charge carriers which limit the hopping of charge carriers from one interstitial site to another. Nonlinear diffusion of the high-resistive element (Al) is responsible for the varying charge carrier concentration. The drift mobility of the prepared samples as a function of temperature is described in Fig 4.

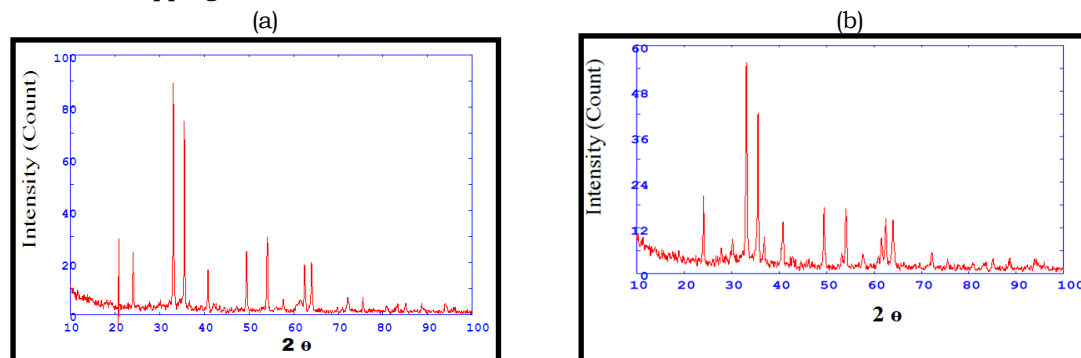


Fig. 1. X-ray diffraction spectra (a) Sample $\text{Ca Al}_1 \text{Fe}_{11} \text{O}_{19}$ and (b) Sample $\text{Ca Al}_3 \text{Fe}_9 \text{O}_{19}$

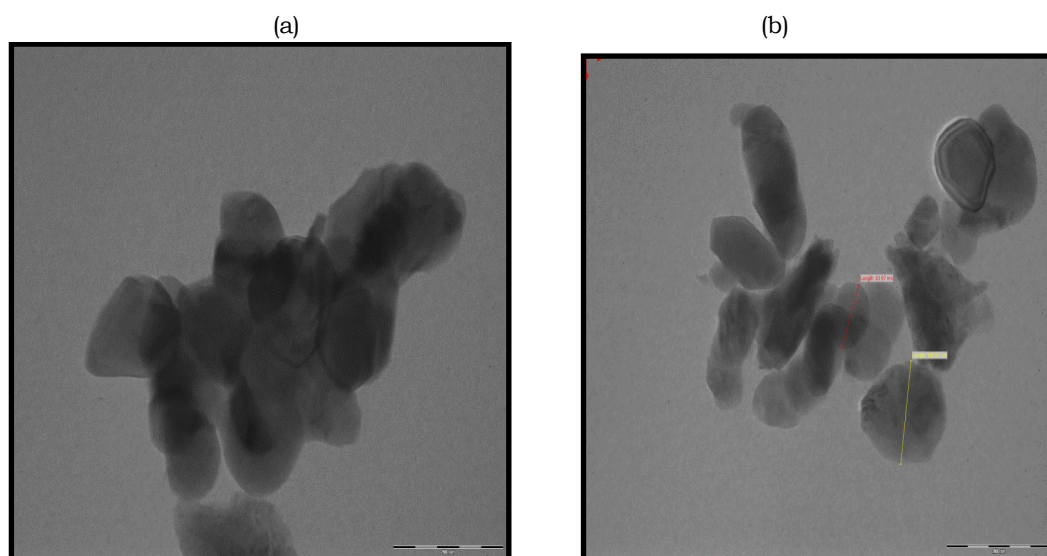


Figure.2: TEM micrographs of samples: (a) $\text{CaAl}_1\text{Fe}_{11}\text{O}_{19}$ and (b) $\text{CaAl}_3\text{Fe}_9\text{O}_{19}$

DC conductivity

Figure. 3 shows the graph of electrical conductivity $\ln(\sigma)$ versus temperature ($10^3/T$) for all ferrites sample.

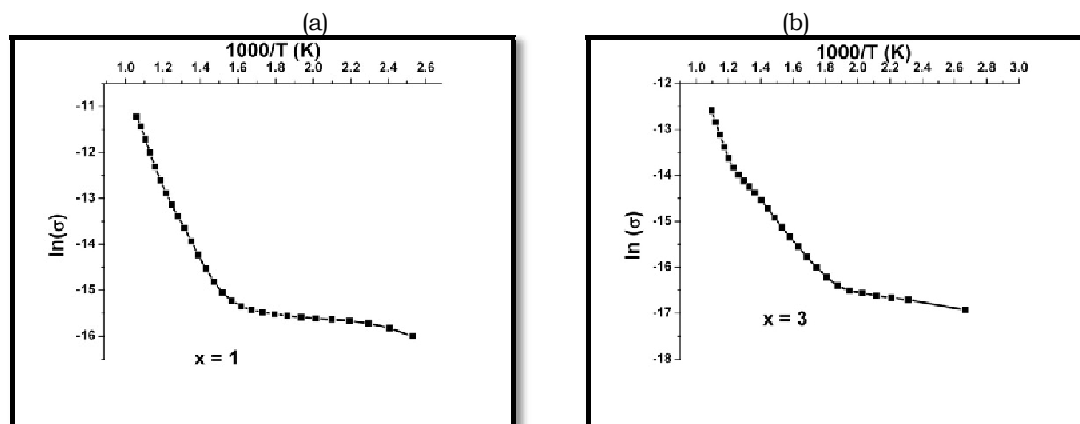


Figure. 3 : Variation of $\ln(\sigma)$ with temperature ($10^3/T$):(a) $\text{CaAl}_1\text{Fe}_{11}\text{O}_{19}$ (b) $\text{CaAl}_3\text{Fe}_9\text{O}_{19}$

Table 1: Lattice constants (a) and (c), cell volume (V), X-ray density ($\rho_{x\text{-ray}}$), Bulk density (ρ_m) and Porosity (P)of Aluminium substituted Calcium hexaferrite.

Sample	A (Å)	c (Å)	V (Å) ³	$\rho_{x\text{-ray}}$ (gm/cm ³)	ρ_m (gm/cm ³)	Porosity P (%)
$\text{CaAl}_1\text{Fe}_{11}\text{O}_{19}$	5.8240	22.1520	650.689	5.029	2.791	45.45
$\text{CaAl}_3\text{Fe}_9\text{O}_{19}$	5.8134	22.1195	647.376	4.734	2.582	47.07

Table 2 : Electrical resistivity and activation energy in Para and Ferri magnetic regions of aluminium substituted calcium ferrite.

Sample	Room Temperature Resistivity ρ (M Ω -cm)	Activation Energy ΔE (eV)	
		Ferri	Para
$\text{CaAl}_1\text{Fe}_{11}\text{O}_{19}$	19.8	0.14	1.51
$\text{CaAl}_3\text{Fe}_9\text{O}_{19}$	22.0	0.72	1.18

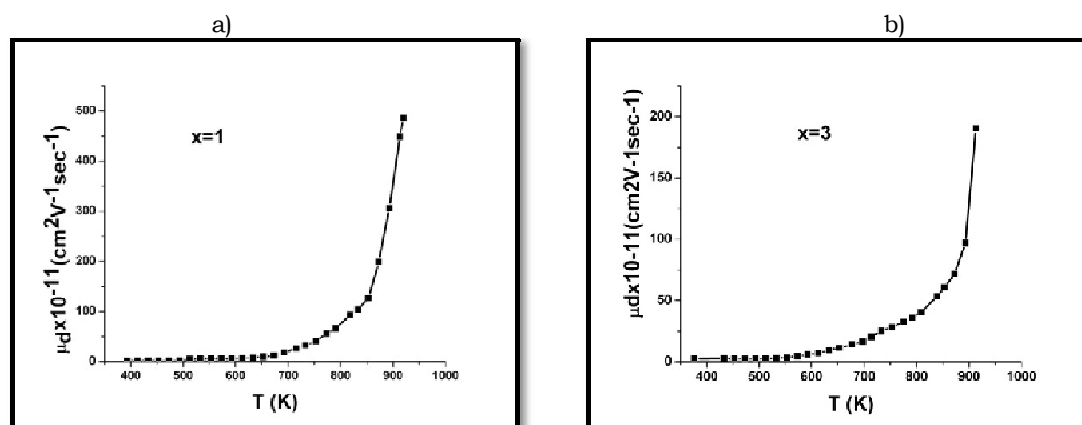


Figure. 4 : Variation of drift mobility (μ_d) with temperature ($10^3/T$):(a) $\text{CaAl}_1\text{Fe}_{11}\text{O}_{19}$ (b) $\text{CaAl}_3\text{Fe}_9\text{O}_{19}$

Conclusion:

The aluminium substituted calcium hexaferrite samples were synthesized by the sol-gel combustion method. The XRD data have confirm the formation of single Phase M-type hexaferrites and the values of a and c of the sample supports this confirmation. TEM studies showed the synthesized samples are in the nano-range. The synthesized samples are semiconductors. The dc electrical resistivity as well as activation energy (E) increased, while the

drift mobility decreased with increasing concentration of Al^{3+} ions. The phenomenon of conduction was explained on the basis of a

Vervey hopping model. The increase in resistivity of the sample with the substitution of Al^{3+} ion for Fe^{3+} ion has potential applications in microwave devices.

References:

[1] Sun C.Q., Prog. Solid State Chem. 35(2007)1

- [2] **Patron L, Mindru I, Marinescu G**, Dekker Encyclopedia of Nanoscience & Nanotechnology, second edition, March 2009.
- [3] **Jacobo S. E, Domingo-pascual C, Rodriguez-clemente R**, J. Mater. Sci. 32 (1997) 1025.
- [4] **Shi P., Yoon D., Zuo X.**, J. Appl. Phys. 87 (2000) 4981.
- [5] **Jain S. R., Adiga K. C. and Pai Verneker V. R.**, Combustion Flame, 40 (1981) 71-79.
- [6] **Kasap S. O.** Principles of Electronic Materials and Devices (New York: McGraw- Hill) (2006).
- [7] **Ounnunkad S., Winotai P.;** J. Magn. Magn. Mater. 301 (2006) 292-300.
- [8] **Haneda K. and Kojima H., Jap.** J. Appl. Phys, 12 (1973) 355.
- [9] **Sang Won Lee, Sung Yong An, In-Bo Shim, Chul Sung Kim**, J. Magn. Magn. Mater. 290 (2005) 231-233.
- [10] **Rewatkar K. G., Patil N. M. and Gawali S. R.**, Bull. Mater. Sci., 28 (6) (2005) 585– 587.
- [11] **The 5th International, Session 5**, New research Trends in Material Science, ARM5, Sibiu, Romania, September (2007) 5-7.
- [12] **Thompson S., Shirtcliffe N. J., Okeefe E.S., Appleton S., Perry C. C.**, J. Magn. Magn. Matter. 292 (2005)100-107.
- [13] **Lakshman A., Rao P. S. V. S., Rao B. P. and Rao K. H.**, J.Phys. D: Appl. Phys. 38 (2005) 673.
- [14] **Kaur B., Bhat M., Licci F., Kumar R., Bamzai K. K. and Kotru P. N.**, J. Mater. Chem. Phys. 103 (2007) 255.
- [15] **Burfoot J. C.** Ferroelectrics: An Introduction to the Physical Principles (London: Van Nostrand) (1967).
- [16] **Molla J., Gonzalez M., Villa R. and Ibara A.** J. Appl. Phys.85 (1999) 1727.
- [17] **Anis-ur-Rehman M., Malik M. A., Khan K. and Maqsood A.**, J. Nano Res. 14 (2011)1.